

Mamba YOLO: SSMs-Based YOLO For Object Detection

Zeyu Wang^{a,1,2}, Chen Li^{a,1,2}, Huiying Xu^{b,1,2}, and Xinzhong Zhu^{b,1,2,3}

¹College of Computer Science and Technology, Zhejiang Normal University, Zhejiang, 311231, China

²Research Institute of Hangzhou Artificial Intelligence, Zhejiang Normal University, Hangzhou, Zhejiang, 311231, China

³Beijing Geekplus Technology Co., Ltd, Beijing, 100101, China

^aThese authors contributed equally to this work.

^bCorresponding authors. Emails: xhy@zjnu.edu.cn, zxz@zjnu.edu.cn

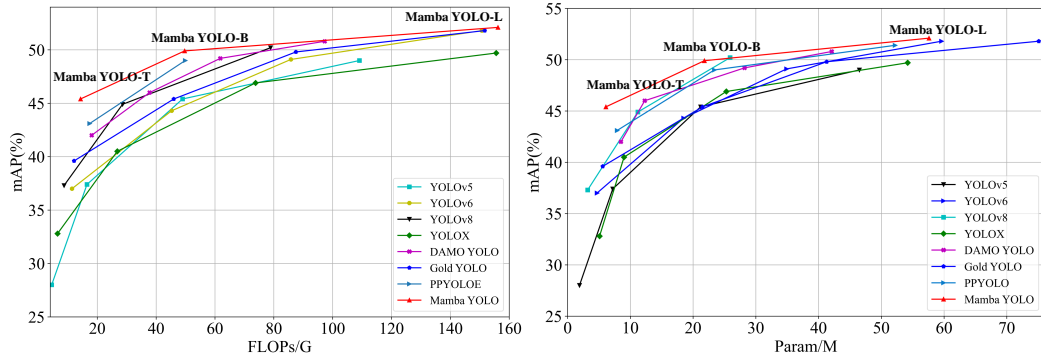


Figure 1: Comparisons of the real-time object detectors on MSCOCO dataset. The object detection method based on SSMs has significant advantages in terms of size-accuracy (right) and FLOPs-accuracy (left).

ABSTRACT

Propelled by the rapid advancement of deep learning technologies, the YOLO series has set a new benchmark for real-time object detectors. Researchers have continuously explored innovative applications of reparameterization, efficient layer aggregation networks, and anchor-free techniques on the foundation of YOLO. To further enhance detection performance, Transformer-based structures have been introduced, significantly expanding the model’s receptive field and achieving notable performance gains. However, such improvements come at a cost, as the quadratic complexity of the self-attention mechanism increases the computational burden of the model. Fortunately, the emergence of State Space Models (SSM) as an innovative technology has effectively mitigated the issues caused by quadratic complexity. In light of these advancements, we introduce Mamba-YOLO a novel object detection model based on SSM. Mamba-YOLO not only optimizes the SSM foundation but also adapts specifically for object detection tasks. Given the potential limitations of SSM in sequence modeling, such as insufficient receptive field and weak image locality, we have designed the LSBlock and RGBlock. These modules enable more precise capture of local image dependencies and significantly enhance the robustness of the model. Extensive experimental results on the publicly available benchmark datasets COCO and VOC demonstrate that Mamba-YOLO surpasses the existing YOLO series models in both performance and competitiveness, showcasing its substantial potential and competitive edge. The PyTorch code is available at: <https://github.com/HZAI-ZJNU/Mamba-YOLO>

1 Introduction

In recent years, deep learning has rapidly advanced, particularly in the field of computer vision, where a series of powerful structures have achieved impressive performance. From CNNs[1, 2, 3, 4, 5] and Transformers[6, 7, 8, 9, 10] to the Mamba architecture [32, 31, 33, 34], the application of various structures has demonstrated their strong potential in computer vision.

In the downstream task of object detection, CNN[15, 16, 17, 20, 21] and Transformer structures [11, 13] are predominantly used. CNNs and their series of improvements offer fast execution speeds while ensuring accuracy. However, due to poor image correlation, researchers have introduced Transformers into the field of object detection, such as the DETR series [11, 12, 14], which relies on the powerful global modeling capabilities of self-attention to address the issue of CNNs' small receptive fields. Fortunately, with hardware advancements, the increased memory computation brought about by this structure does not pose too much of a problem. But, in recent years, more work [5, 59, 60] has begun to rethink how to design CNNs to make models faster, and more practitioners are becoming dissatisfied with the quadratic complexity of Transformer structures, starting to use hybrid structures to reconstruct models and reduce complexity, such as MobileVit [61], EdgeVit [62], EfficientFormer [43]. However, hybrid models also bring problems, and the apparent decline in performance is also a concern, so finding a balance between performance and speed has always been a concern for researchers.

YOLO series has always been a milestone real-time detector in the field of object detection. Starting with YOLOv4 [25], CSPNet [63] was introduced, YOLOv6 [27] began to incorporate reparameterization, YOLOv7 [28] used ELAN to rebuild the model, and YOLOv8 [42] employed a decoupled head and anchor-free design. The recently proposed YOLOv10 [48] integrated elements of the Transformer structure into its design, introducing the Partial Self-Attention (PSA) module, aimed at enhancing the model's global modeling capabilities while controlling computational costs. This proves that this series has always had strong vitality. Moreover, the structure of CNNs gives the model a powerful execution speed, and many practitioners have used attention mechanisms to improve this model to achieve desired performance improvements in their field.

ViT-YOLO [38] introduced MHSA-Darknet into YOLO, along with enhanced training strategies such as TTA and weighted frame fusion techniques. However, the increase in the number of parameters and FLOPs did not lead to the expected performance improvement, showing the limitations of Transformer scalability in object detection tasks, especially in YOLO. YOLOs [37] adopted a minimalist retrofit scheme based on the original ViT architecture, replacing the CLS markers in ViT with DET markers and employing dichotomous matching loss in an ensemble prediction approach. However, its performance was disappointing, and it was very sensitive to the pre-training scheme, with YOLOs showing great variability under different pre-training strategies. Gold-YOLO [29] proposed a method to enhance the fusion of multi-scale features by extracting and fusing feature information through convolutional and attention primitives. However, these methods, while integrating the Transformer structure, abandoned its core advantages, namely the powerful global attention mechanism and long sequence processing capability, and yet sought to reduce the computational surge brought by the reduction of quadratic complexity, which often limited the model's performance.

Recently, methods based on state space models (SSMs), such as Mamba [32], have provided new ideas for solving these problems due to their strong modeling capabilities for long-distance dependencies and superior properties of linear time complexity. It is exciting that researchers have successfully introduced the Mamba architecture into the visual domain and achieved success in image classification [31, 33]. Inspired by this, we bring forth a question: *Can the SSM structure be introduced into the field of object detection, combined with current real-time detectors, to benefit from the advantages of SSM and bring new performance improvements to the YOLO series?*

This paper proposes a detector model called Mamba-YOLO. We have introduced the ODSSBlock module, as shown in Figure 4, applying the SSM structure to the field of object detection. Unlike the VSSBlock for image classification, the images inputted for object detection have larger pixels, and since the SSM model typically models text sequences, lacking channel expression capability for images, we have proposed the LSBlock to model channel features. Benefiting from the larger pixels and more dimensions of channels in images, we have proposed the RGBlock structure to further decode after the SS2D output, using the high-dimensional expression of dot multiplication to improve channel correlation. Mamba-YOLO is an important advancement in visual recognition and detection tasks, aiming to build a novel backbone network that combines the advantages of SSM and CNN. The architecture applies SSM-based state-space transition models to the layers of YOLO to effectively capture global dependencies and utilize the strength of local convolutions to improve detection accuracy and the model's understanding of complex scenes while maintaining real-time performance. Such a hybrid architecture is expected to break through the limitations of existing vision models in processing large-scale or high-resolution images and provide powerful and flexible support for next-generation vision base models. We have conducted exhaustive experiments on PASCAL VOC[35], COCO[36], and the results show that Mamba-YOLO is very competitive in general object detection tasks, achieving a mAP that is 8.1% higher than the baseline YOLOv8 on MSCOCO.

The main contributions of this paper can be summarized as follows:

- We propose Mamba-YOLO, which is based on the SSM, establishes a new baseline for YOLOs in object detection, and lays a solid foundation for the future development of more efficient and effective detectors based on the SSM.
- We propose ODSSBlock, in which the LS Block effectively extracts the local spatial information of the input feature maps to compensate the local modeling capability of SSM. By rethinking the design of the MLP layer, we propose the RG Block by combining the idea of gated aggregation with effective convolution with residual connectivity, which effectively captures local dependencies and enhances model robustness.

- We designed a set of models Mamba-YOLO (Tiny/Base/Large) with different scales to support the deployment of tasks with different sizes and scales, and conducted experiments on two datasets, COCO and VOC , as shown in Figure 1, which show that our Mamba-YOLO achieves a significant performance improvement compared to existing state-of-the-art approaches.

2 Related Work

2.1 Real-time Object Detectors

YOLOv1 to YOLOv3 [22, 23, 24] are the pioneers of YOLO-series models, and their performance improvements are all closely related to the backbone improvement and make DarkNet widely used. YOLOv4[25]introduces a large number of residual structure design proposed CSPDarknet53 backbone network, which effectively reduces computational redundancy and realizes high-performance feature expression and efficient training. YOLOv7 [28] proposes the E-ELAN structure to enhance the model capability without destroying the original . Yolov8[42] combines the features of the previous generations of YOLOs and adopts the C2f structure with richer gradient streams, which is lightweight and adaptable to different scenarios while taking accuracy into account. Recently, Gold Yolo [29] introduced a new mechanism named GD (Gather-and-Distribute), which is realized by self-attention operation to solve the problem of information fusion of traditional feature pyramid networks [52] and Rep-PAN [27], and succeeded in achieve the SOTA. In fact, traditional CNNs have certain limitations on the challenges of drastic scale changes, complex background and multi-view interference in images due to their local receptive fields and hierarchical structure design.

2.2 End-to-end Object Detectors

DETR[11]introduces Transformer to object detection for the first time, using a transformer encoder-decoder architecture that bypasses traditional handcrafted components like anchor generation and non-maximum suppression, treating detection as a straightforward ensemble prediction problem. Deformable DETR[12] introduces Deformable Attention, a variant of Transformer Attention for sampling a sparse set of keypoints around a reference location, addressing the limitations of DETR in handling high-resolution feature maps. DINO [13] integrates a hybrid query selection strategy, deformable attention and demonstrated training with injected noise and performance improvement through query optimization. RT-DETR [14] proposed a hybrid encoder to decouple intra-scale interactions and cross-scale fusion for efficient multi-scale feature processing. However, DETRs have challenges in training convergence, computational cost, and small target detection, and YOLO-series remains the SOTA with balanced accuracy and speed in the small model domain.

2.3 Vision State Space Models

Recently, State Space Models are the hotspot of recent research. Based on the study of SSM [39, 40, 41], Mamba[32] shows linear complexity in input size, and solves the computational efficiency problem of Transformer on long sequences of modeling state space. In the field of generalized visual backbone, Vision Mamba [33] proposed a pure visual backbone model based on SSM, marking the first time that Mamba has been introduced into the field of vision. VMamba [31] introduced the Cross-Scan module to enable the model to 2D image Selective scanning enhances visual processing and demonstrates superiority on image classification tasks. LocalMamba [34] focuses on window scanning strategies for visuospatial models, optimizes visual information to capture local dependencies, and introduces dynamic scanning methods to search for optimal choices for different layers. MambaOut[49] explores the necessity of Mamba architecture in vision tasks, it states that SSM is not necessary for image classification tasks, but its value for detection and segmentation tasks that follow long sequence characteristics is worth exploring further.In downstream vision tasks, Mamba has also been widely used in research on medical image segmentation[53, 54, 55] and remote sensing image segmentation[56, 57]. Inspired by the remarkable results achieved by VMamba [31]in the field of visual tasks,this paper presents for the first time mamba YOLO, a new SSMs model that aims to take into account the global sensory field while demonstrating its potential in object detection tasks.

3 Method

3.1 Preliminaries

The structured state-space sequence models S4 [39]and Mamba[32] , rooted in State Space Model(SSM), both stem from a continuous system that maps a univariate sequence $x(t) \in \mathbb{R}$ into an output sequence $y(t)$ via an implicit latent intermediate state $h(t) \in \mathbb{R}^N$. This design not only bridges the relationship between inputs and outputs but also encapsulates temporal dynamics. The system can be mathematically defined as follows:

$$h'(t) = \mathbf{A}h(t) + \mathbf{B}x(t) \tag{1}$$

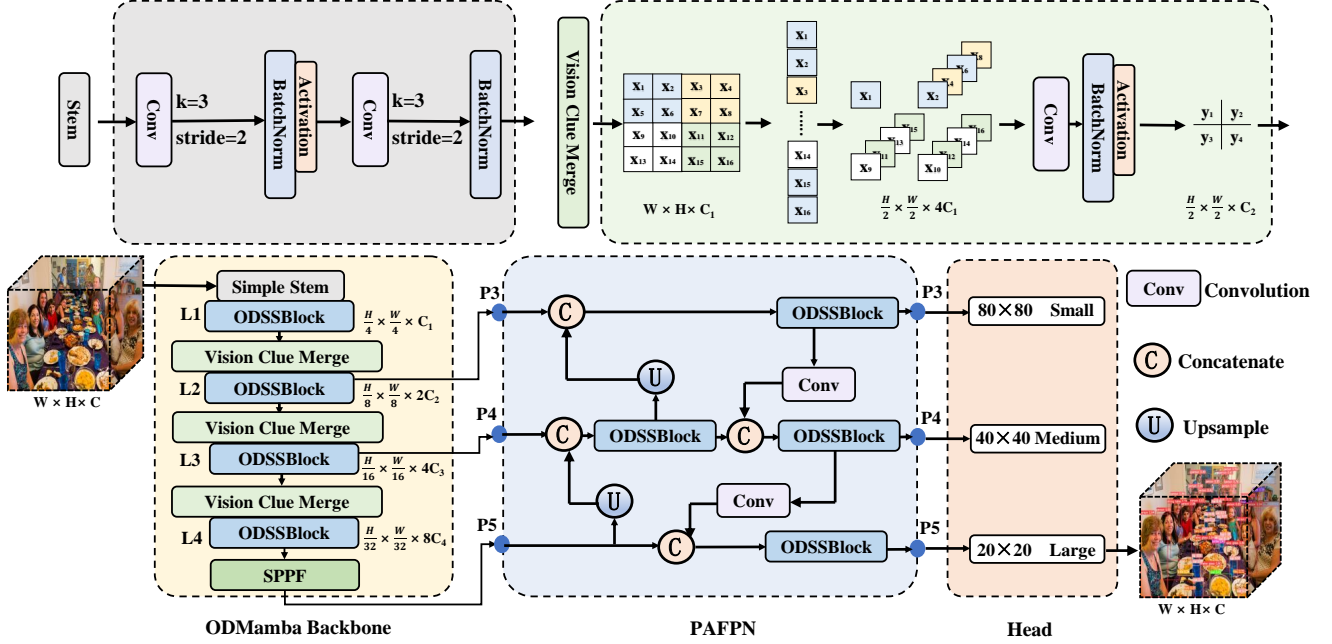


Figure 2: Illustration of Mamba YOLO architecture.

$$y(t) = Ch(t) \quad (2)$$

In Equation (1), $\mathbf{A} \in \mathbb{R}^{N \times N}$ represents the state transition matrix, which governs how the hidden state evolves over time, while $\mathbf{B} \in \mathbb{R}^{N \times 1}$ denotes the weight matrix for the input space in relation to the hidden state. Moreover, $\mathbf{C} \in \mathbb{R}^{N \times 1}$ is the observation matrix, which maps the hidden intermediate state to the output. Mamba applies this continuous system to discrete-time sequence data by employing fixed discretization rules f_A and f_B to transform the parameters \mathbf{A} and \mathbf{B} into their discrete counterparts $\bar{\mathbf{A}}$ and $\bar{\mathbf{B}}$, respectively, thereby better integrating the system into deep learning architectures. A commonly used discretization method for this purpose is the Zero-Order Hold (ZOH). The discretized version can be defined as follows:

$$\bar{\mathbf{A}} = \exp(\Delta \mathbf{A}) \quad (3)$$

$$\bar{\mathbf{B}} = (\Delta \mathbf{A})^{-1} (\exp(\Delta \mathbf{A}) - \mathbf{I}) \Delta \mathbf{B} \quad (4)$$

In Equation (4), Δ represents a time scale parameter that adjusts the temporal resolution of the model, and ΔA and ΔB correspondingly denote the discrete-time counterparts of the continuous parameters over the given time interval. Here, \mathbf{I} represents the identity matrix. After transformation, the model computes via linear recursive forms, which can be defined as follows:

$$h'(t) = \bar{\mathbf{A}} h_{t-1} + \bar{\mathbf{B}} x_t \quad (5)$$

$$y_t = Ch_t \quad (6)$$

The entire sequence transformation can also be represented in a convolutional form, which is defined as follows:

$$\bar{\mathbf{K}} = (\bar{\mathbf{C}}\bar{\mathbf{B}}, \bar{\mathbf{C}}\bar{\mathbf{A}}\bar{\mathbf{B}}, \dots, \bar{\mathbf{C}}\bar{\mathbf{A}}^{L-1}\bar{\mathbf{B}}) \quad (7)$$

$$y = x * \bar{\mathbf{K}} \quad (8)$$

Wherein, $\bar{\mathbf{K}} \in \mathbb{R}^L$ represents the structured convolutional kernel, with L denoting the length of the input equence. In the design presented in this paper, the model employs a convolutional form for parallel training and utilizes a linear recursive formulation for efficient autoregressive inference.

3.2 Overall Architecture

An overview of the architecture of Mamba YOLO is illustrated in Figure 2. Our object detection model is divided into the ODMamba backbone and neck parts. ODMamba consists of the Simple Stem, Downsample Block. In the neck, we follow the design of PAN-FPN using the ODSSBlock module instead of C2f[42] to capture a more gradient-rich information flow. The backbone first undergoes downsampling through a Stem module, resulting in a 2D feature map with a resolution of $\frac{H}{4}, \frac{W}{4}$. Subsequently, all models consist of ODSSBlock followed by a VisionClue Merge module for further downsampling. In the neck part, we adopt the design of PAFPN[42], using ODSSBlock to replace C2f, where Conv is solely responsible for downsampling.

Simple Stem Modern Vision Transformers (ViTs) typically employ segmented patches as their initial modules, dividing the image into non-overlapping segments. This segmentation process is achieved through a convolutional operation with a kernel size of 4 and a stride of 4. However, recent research, such as that from EfficientFormerV2[43], suggests that this approach may limit the optimization capabilities of ViTs, impacting overall performance. To strike a balance between performance and efficiency, we propose a streamlined stem layer. Instead of using non-overlapping patches, we employ two convolutions with a stride of 2 and a kernel size of 3.

Vision Clue Merge While Convolutional Neural Networks (CNNs) and Vision Transformer (ViT) structures commonly employ convolutions for downsampling, we discovered that this approach interferes with the selective operation of SS2D[31] across different information flow stages. To address this, VMamba[31] splits the 2D feature map and reduces dimensions using 1x1 convolutions. Our findings indicate that preserving more visual clues for State Spaces Models (SSMs) benefits model training. In contrast to the conventional halving of dimensions, we streamline this process by: 1) Removing the norm; 2) Splitting the dimension map; 3) Appending excess feature maps to the channel dimension; 4) Utilizing a 4x compressed pointwise convolution for downsampling. Unlike the use of a 3x3 convolution with a stride of 2, our method preserves the feature map selected by SS2D from the previous layer.

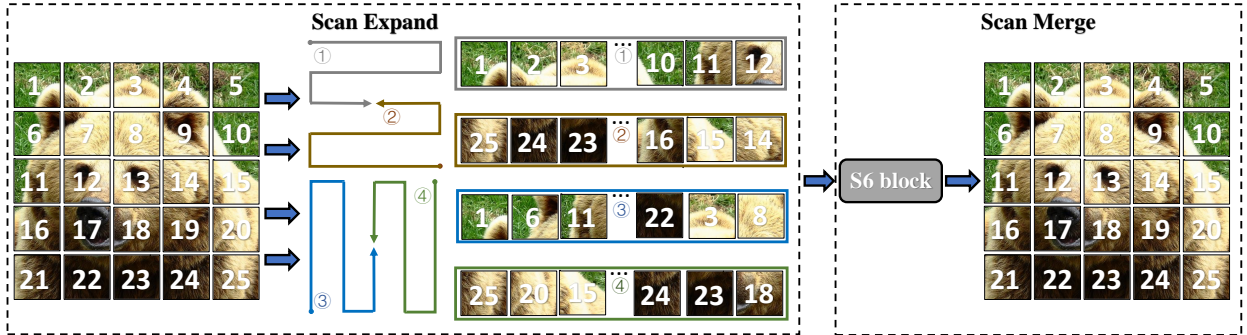


Figure 3: Illustration of the SS2D operation. The scan expansion operation in SS2D is divided into four branches that scan the image block by block in four different directional paths of the image and obtain four sequences. The scan merge operation in SS2D takes the obtained sequences as inputs to the S6 block and merges the sequences from the different directions so that the features are extracted to the global features.

3.3 ODSS Block

As shown in Figure 4, ODSS Block is the core module of Mamba YOLO, which undergoes a series of processing in the input stage to enable the network to learn deeper and richer feature representations, while keeping the training inference process efficient and stable through batch normalization.

$$Z^{l-2} = \hat{\Phi}(BN(Conv_{1 \times 1}(Z^{l-3})) \quad (9)$$

Where $\hat{\Phi}$ denotes the activation function (nonlinear SiLU). The Layer Normalization and Residual Linking design of the ODSS Block draws on a Transformer Blocks[6] style architecture, which allows the model to flow efficiently in the presence of deep stacking. and training in the case of deep stacking. The calculation formula is as follows:

$$Z^{l-1} = SS2D(LN(LS(Z^{l-2}))) + Z^{l-2} \quad (10)$$

$$Z^l = RG(LN(Z^{l-1})) + Z^{l-1} \quad (11)$$

Where Z^{l-3} and Z^l denote the input and output features, LS and RG denote **LocalSpatial Block** and **ResGated Block**, respectively, and Z^{l-1} denotes the intermediate state after 2D-Selective-Scan[31]. Scan Expansion, S6 Block and Scan Merge are the three main steps of the SS2D[31] algorithm, and its main flow is shown in Figure 3. The scan expansion operation expands the input image into a series of subimages, each of which denotes a specific direction, and when observed from the diagonal viewpoint, the scan expansion operation proceeds along the four symmetric directions, which are top-down, bottom-up, left-right, and word-right-to-left, respectively. Such a layout not only comprehensively covers all regions of the input image, but also enhances the efficiency and comprehensiveness of multi-dimensional capturing of image features by providing a rich multi-dimensional information base for subsequent feature extraction through systematic direction transformation. Then these sub-images are subjected to feature extraction in the S6 block[32] operation, and finally by the scanning merge operation, these sub-images are merged together to form an output image of the same size as the input image.

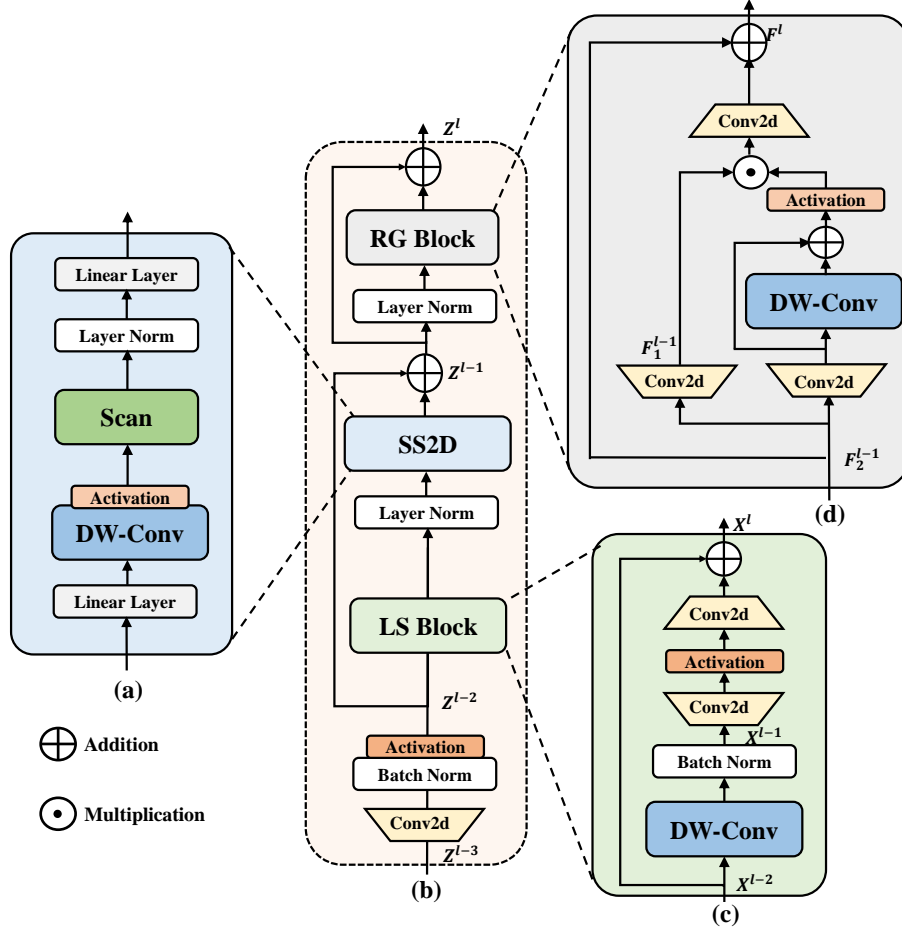


Figure 4: (a)Detailed Structure of the SS2D (b) Illustration of ODSSBlock architecture.(c)Illustration of Residual Gated Block(RGBlock)(d)Illustration of Local Spatial Block(LSBlock)

3.3.1 LocalSpatial Block

The Mamba architecture has been proven to be effective in capturing long-range ground dependencies. However, it faces certain challenges in extracting local features when dealing with tasks involving complex scale variations. In Figure 4(c), this paper proposes LocalSpatial Block to enhance the capture of local features. Specifically, for a given input feature $F^{l-1} \in \mathbb{R}^{C \times H \times W}$, it first undergoes depth-separable convolution, which operates on each input channel individually without mixing the channel information. The local spatial information of the input feature map is effectively extracted, while reducing the computational cost and the number of parameters, and then undergoes Batch Normalization to provide a certain degree of regularization effect while reducing the overfitting, the obtained intermediate state F^{l-1} is defined as:

$$F^{l-1} = BN(DWConv_{3 \times 3}(F^{l-2})) \quad (12)$$

The intermediate state F^{l-1} mixes the channel information by a 1×1 convolution and better preserves the distribution of the information through the activation function, enabling the model to learn more complex feature representations that are able to extract rich multi-scale contextual information from the input feature maps. In LSBlock, the activation function uses a nonlinear GELU to change the number of channels of the features without changing the spatial dimension, thus enhancing the feature representation. Finally, the original inputs are fused with the processed features through residual concatenation. Allows the model to understand and integrate features of different dimensions in the image, thus enhancing robustness to scale changes.

$$F^l = Conv_{1 \times 1}(\Phi(Conv_{1 \times 1}(F^{l-1}))) \oplus F^{l-2} \quad (13)$$

Where F^l is the output feature and Φ denotes the activation function. LSBlock is able to efficiently capture and represent the local spatial information of the input feature map and fuse it with the original input to enhance the representation of the features, providing Mamba YOLO with a powerful capability to handle scale variations and contextual information in visual data.

3.3.2 ResGated Block

The original MLP is still the most widely adopted, and the MLP in VMamba[31] architecture also follows the Transformer design, which performs nonlinear transformations on the input sequences to enhance the expressive power of the model. Recent studies, Gated MLP[44, 45] shows strong performance in natural language processing, and we find that the mechanism of gating has the same potential for vision. In Figure 4(d), this paper proposes that the simple design of ResGated Block aims to improve the performance of the model with low computational cost, RG Block creates two branches X_1^{l-1} and X_2^{l-1} from the input X^{l-2} and implements the fully-connected layer in the form of a 1×1 convolution on each branch.

$$X_1^{l-1} = Conv_{1 \times 1}(X^{l-2}) \quad (14)$$

$$X_2^{l-1} = Conv_{1 \times 1}(X^{l-2}) \quad (15)$$

Depth separable convolution is used as the Position Encoding Module on the branch of X_2^{l-1} , and the gradient is more efficiently refluxed during training by means of residual concatenation, which has a lower computational cost and significantly improves the performance by preserving and utilizing the spatial structural information of the image. The RG Block adopts a nonlinear GeLU as an activation function to control the flow of information at each level, then merged with a branch of X_2^{l-1} through elemental multiplication, then refined with global features through a 1×1 convolution to blend the channel information, and finally summed with the original input X^{l-2} with the features in the hidden layer through residual concatenation. RG Block can capture more global features while bringing only a slight increase in computational cost, the resulting output features X^l are defined as:

$$X^l = Conv_{1 \times 1}(X_1^{l-1} \odot \Phi(DWConv_{3 \times 3}(X_2^{l-1}) \oplus X_2^{l-1})) \oplus X^{l-2} \quad (16)$$

Where Φ denotes the activation function (nonlinear GeLU). In this paper, the gating mechanism in RG Block preserves the spatial information by integrating the convolution operation while making the model more sensitive to the fine-grained features in the image. Compared with the traditional MLP, RG Block transfers the global dependencies and global features to each pixel to capture the dependencies of the neighboring features, which makes the contextual information rich to further enhance the model's expressive ability.

4 Experiments

In this section, we conduct comprehensive experiments on Mamba YOLO for object detection task and some downstream vision tasks. We employ the MS COCO[36] dataset to validate the superiority of the proposed Mamba YOLO. Comparison with state-of-the-arts, we train on the COCO2017train dataset and validate on the COCO2017val dataset. In the ablation experiments, the effectiveness of each of the proposed methods is validated with the VOC0712[35] dataset, where the training set contains about 16,551 images from the VOC2007 and VOC2012 training sets, and the validation set consists of 4,952 images from the VOC2007 test set. All the models we mentioned were trained using the strategy of training from scratch and the total number of training sessions was 500. For more setups more setups please refer to the Appendix. All our models are trained on 8 NVIDIA H800 GPUs.

4.1 Comparison with state-of-the-arts

Fig1 and Table 1 show the results of MS-COCO2017val compared to other state-of-the-art object detectors, where the method proposed in this paper has the best combined trade-off between FLOPs and Params and accuracy. Specifically, Mamba YOLO-T

Table 1: The comparison of Mamba YOLO with other detectors from the YOLO series on the COCO 2017 val

Method	$AP^{val}(\%)$	$AP_{50}^{val}(\%)$	$AP_{75}^{val}(\%)$	$AP_S^{val}(\%)$	$AP_M^{val}(\%)$	$AP_L^{val}(\%)$	#param.	FLOPs
YOLOv5-N[46]	28.0	45.7	-	-	-	-	1.9 M	4.5 G
YOLOv5-S[46]	37.4	56.8	-	-	-	-	7.2 M	16.5 G
YOLOv5-M[46]	45.4	64.1	-	-	-	-	21.2 M	49.0 G
YOLOv5-L[46]	49.0	67.3	-	-	-	-	46.5 M	109.1 G
YOLOv6-3.0-N[27]	37.0	52.7	-	-	-	-	4.7 M	4.7 G
YOLOv6-3.0-S[27]	44.3	61.2	-	-	-	-	4.7 M	45.3 G
YOLOv6-3.0-M[27]	49.1	66.1	-	-	-	-	85.8 G	85.8 G
YOLOv6-3.0-L[27]	51.8	69.2	-	-	-	-	59.6 M	150.7 G
YOLOv7-Tiny[28]	37.4	55.2	37.3	15.7	38.0	53.4	6.2 M	13.7 G
YOLOv7[28]	51.2	69.7	55.9	31.8	55.5	65.0	36.9 M	104.7 G
YOLOv7-X[28]	52.9	71.7	51.4	36.9	57.7	68.6	71.3 M	189.9 G
YOLOv8-N[42]	37.3	52.6	40.6	18.8	41.0	53.5	3.2 M	8.7 G
YOLOv8-S[42]	44.9	61.8	48.6	26.0	49.9	61.0	11.2 M	28.6 G
YOLOv8-M[42]	50.2	67.3	54.8	32.3	55.9	66.5	25.9 M	78.9 G
YOLOv8-L[42]	52.9	69.8	57.7	35.5	58.5	69.8	43.7M	165.2 G
DAMO YOLO-T[30]	42.0	58.0	45.2	23.0	46.1	58.5	8.5 M	18.1 G
DAMO YOLO-S[30]	46.0	61.9	49.5	25.9	50.6	62.5	12.3 M	37.8 G
DAMO YOLO-M [30]	49.2	65.5	53.0	29.7	53.1	66.1	28.2 M	61.8 G
DAMO YOLO-L[30]	50.8	67.5	55.5	33.2	55.7	66.6	42.1 M	97.3 G
Gold-YOLO-N [29]	39.6	55.7	-	19.7	44.1	57.0	5.6 M	12.1 G
Gold-YOLO-S [29]	45.4	62.5	-	25.3	50.2	62.6	21.5 M	46.0 G
Gold-YOLO-M [29]	49.8	67.0	-	32.3	55.3	66.3	41.3 M	87.5 G
Gold-YOLO-L [29]	51.8	68.9	-	34.1	57.4	68.2	75.1 M	151.7 G
YOLO MS-XS [47]	43.4	60.4	47.6	23.7	48.3	60.3	4.5 M	17.4G
YOLO MS-S [47]	46.2	63.7	50.5	26.9	50.5	63.0	8.1 M	31.2 G
YOLO MS [47]	51.0	68.6	55.7	33.1	56.1	66.5	22.2 M	80.2 G
Mamba YOLO-T	45.4	62.3	49.1	25.2	50.4	62.9	6.1M	14.3G
Mamba YOLO-B	49.9	67.2	54.4	30.6	55.4	67.0	21.8M	49.7G
Mamba YOLO-L	52.1	69.8	56.5	34.1	57.3	68.1	57.6 M	156.2G

has a significant 3.4%/2.0% increase in AP compared to the best performing tiny lightweight model DAMO YOLO-T/YOLO MS-XS, and a 45.5% reduction in Params and a 50% reduction in FLOPs compared to the baseline YOLOv8-S, which has about the same accuracy. Comparing the Mamba YOLO-B to the Gold-YOLO-M, which has similar Params and FLOPs, the AP gain of the former is 4.5% higher than that of the latter. Even compared to Gold-YOLO-M with the same accuracy, Params are reduced by 47.2% and FLOPs by 43.2%. In large models, Mamba YOLO-L also achieves better or similar performance compared to each of the advanced object detectors. Compared with the best-performing Gold-YOLO-L, the AP of Mamba YOLO-L increased by 0.3%, while the Params decreased by 0.9%. The above comparative results show that our proposed model provides significant improvements at different scales of Mamba YOLO compared to the existing state-of-the-art methods.

4.2 Ablation study

4.2.1 Ablation study on Mamba YOLO

In this section, we examine each module in the ODSS Block independently, and without Clue Merge, we downsample using the traditional convolutional method of Vision Transformers to assess the impact of Vision Clue Merge on accuracy. Mamba YOLO is performed on the VOC0712 dataset to conduct Ablation experiments, and the test model is Mamba YOLO-T. Table 2 of our results shows that cue merging preserves more visual cues for the state-space model (SSM) and also provides evidence for the assertion that the ODSS block structure is indeed optimal.

Table 2: Ablation study on Mamba YOLO

Model	ODSSBlock		Clue Merge	mAP	mAP50
	LS Block	RG Block			
1				57.0	77.4
2	✓			57.8	78.1
3		✓		58.1	78.4
4			✓	57.1	77.6
5	✓	✓		58.4	78.5
6	✓	✓	✓	58.7	78.6

4.2.2 Ablation study on RG Block structure

RGBlock to capture pixel-by-pixel local dependencies by taking global dependencies and global features from pixel-by-pixel. Regarding the details of the RG Block design, we also consider three variants on top of the Multi-Layer Perception base: 1) Convolutional MLP, which adds DW-Conv to the original MLP; 2) Res-Convolutional MLP, which adds DW-Conv in a residual concatenated fashion added to the original MLP; 3) Gated MLP, an MLP variant designed under the gating mechanism. Figure 5 illustrates these variants, and Table 3 shows the performance of the original MLP, RG Block, and each variant in the VOC0712 dataset to verify the validity of our analysis on the MLP, with the test model Mamba YOLO-T. We observe that the introduction of convolution singly does not lead to an effective improvement in the performance, whereas in the variant Figure 5(d) Gated MLP, the Its output consists of two linear projections of element multiplication, one of which consists of residual-connected DWConv and gated activation functions, which in fact endows the model with the ability to propagate important features through the hierarchical structure and effectively improves the accuracy and robustness of the model. This experiment shows that the improvement of the performance of the introduced convolution when dealing with complex image tasks is quite relevant to the gated aggregation mechanism, provided that they are applied in the context of residual connectivity.

Table 3: Ablation study on MPL variants and RG Block.

Model	mAP	mAP50
Original MLP	57.1	77.6
Convolutional MLP	57.5	77.8
Res-Convolutional MLP	57.9	78.1
Gated MLP	58.1	78.2
RG Block(Ours)	58.1	78.4

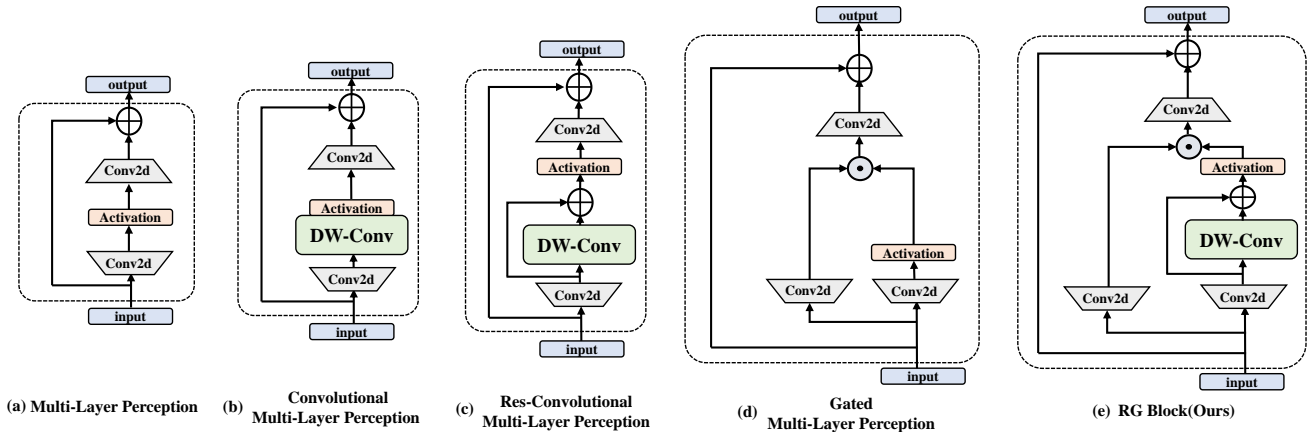


Figure 5: RG Block integration designs explored in the ablation study.

4.2.3 Ablation study on other model and Instance Segmentation

To evaluate the superiority and good scalability of our proposed ssm-based Mamba YOLO architecture, we apply it to instance segmentation tasks in addition to the target detection domain. We adopt the v8 segmentation head [42] on top of Mamba YOLO-T and train and test it on the COCOseg dataset, evaluating the model performance by metrics such as Bbox AP and Mask AP. The Mamba YOLO-T-seg dramatically outperforms the segmentation models of YOLOv5 [46] and YOLOv8 [42] for each size. RTMDet[58], based on a basic building block containing a large kernel of deep convolution, introduces soft labels to compute the matching cost during the dynamic label assignment process, and shows excellent performance in several visual tasks, and the Mamba YOLO-T-seg still manages to maintain an advantage of 2.3 on Mask mAP compared to its Tiny. The results are shown in Table 4 and Figure 8.

Table 4: Ablation study on Instance Segmentation with v8Head

Model	Bbox mAP	Bbox mAP50	Mask mAP	Mask mAP50	Params/M	FLOPs/G
YOLOv5-N-seg[46]	27.6	-	23.4	-	2.0	7.1
YOLOv5-S-seg [46]	37.6	-	31.7	-	7.6	26.4
YOLOv8-N-seg [42]	36.2	51.2	29.6	48.2	3.4	12.6
YOLOv8-S-seg [42]	44.0	60.4	36.0	56.8	11.8	42.6
RTMDet-Ins-Tiny [58]	40.5	-	35.4	-	5.6	11.8
RTMDet-Ins-S [58]	44.0	-	38.7	-	10.18	21.5
Mamba YOLO-T-seg	45.1	61.3	36.7	57.8	7.0	18.1

5 Conclusion

In this paper, we reanalyze the advantages and disadvantages of CNN and Transformer architectures in the field of object detection and point out the limitations of their fusion. Based on this, we propose a detector designed based on the state space models architecture and extended by YOLO, we re-analyze the limitations of the traditional MLP and propose the RG Block, whose gating mechanism and deep convolutional residual connectivity are designed to give the model the ability to propagate important features in the hierarchical structure. In addition, to address the limitations of the Mamba architecture in capturing local dependencies, LSBlock enhances the ability to capture local features and fuses them with the original inputs to enhance the representation of the features, which significantly improves the model’s detection capability. Our goal is to establish a new baseline of YOLOs, proving that Mamba YOLO are highly competitive. Our work is the first exploration of the Mamba architecture in the real-time object detection task, and we also hope to bring new ideas to researchers in the field.

6 Acknowledgments

This work was supported by the National Natural Science Foundation of China under contract 61976196 and the Key Project of the Natural Science Foundation of Zhejiang Province under contract LZ22F030003.

References

- [1] Karen Simonyan and Andrew Zisserman. Very deep convolutional networks for large-scale image recognition. In *arXiv preprint arXiv:1409.1556*, 2015.
- [2] Kaiming He, Xiangyu Zhang, Shaoqing Ren, and Jian Sun. Deep residual learning for image recognition. In *arXiv preprint arXiv:1512.03385*, 2015.
- [3] Gao Huang, Zhuang Liu, Laurens van der Maaten, and Kilian Q. Weinberger. Densely connected convolutional networks. In *Proceedings of the IEEE Conference on Computer Vision and Pattern Recognition*, 2017.
- [4] Mingxing Tan and Quoc V. Le. EfficientNetV2: Smaller Models and Faster Training. In *Proceedings of the International Conference on Machine Learning*, pages 10096–10106. PMLR, 2021.
- [5] Zhuang Liu, Hanzi Mao, Chao-Yuan Wu, Christoph Feichtenhofer, Trevor Darrell, and Saining Xie. A convnet for the 2020s. In *Proceedings of the IEEE/CVF Conference on Computer Vision and Pattern Recognition (CVPR)*, 2022.
- [6] Alexey Dosovitskiy, Lucas Beyer, Alexander Kolesnikov, et al. An Image is Worth 16x16 Words: Transformers for Image Recognition at Scale. In *arXiv preprint arXiv:2010.11929*, 2020.

- [7] Ze Liu, Yutong Lin, Yue Cao, Han Hu, Yixuan Wei, Zheng Zhang, Stephen Lin, and Baining Guo. Swin Transformer: Hierarchical Vision Transformer using Shifted Windows. In *Proceedings of the IEEE/CVF International Conference on Computer Vision (ICCV)*, 2021.
- [8] Hugo Touvron, Matthieu Cord, Matthijs Douze, et al. Training Data-Efficient Image Transformers & Distillation Through Attention. In *International conference on machine learning*, PMLR, pages 10347–10357, 2021.
- [9] Xiaosong Zhang, Yunjie Tian, Wei Huang, Qixiang Ye, Qi Dai, Lingxi Xie, and Qi Tian. HiViT: Hierarchical Vision Transformer Meets Masked Image Modeling. In *arXiv preprint arXiv:2205.14949*, 2022.
- [10] Dai Shi. TransNeXt: Robust Foveal Visual Perception for Vision Transformers. In *arXiv preprint arXiv:2311.17132*, 2023.
- [11] Nicolas Carion, Francisco Massa, Gabriel Synnaeve, Nicolas Usunier, Alexander Kirillov, and Sergey Zagoruyko. End-to-End Object Detection with Transformers. In *a European conference on computer vision. Cham: Springer International Publishing(ECCV)*, 2020.
- [12] Xizhou Zhu, Weijie Su, Lewei Lu, Bin Li, Xiaogang Wang, and Jifeng Dai. Deformable DETR: Deformable Transformers for End-to-End Object Detection. In *arXiv preprint arXiv:2010.04159*, 2020.
- [13] Hao Zhang, Feng Li, Shilong Liu, Lei Zhang, Hang Su, Jun Zhu, Lionel M. Ni, and Heung-Yeung Shum. DINO: DETR with Improved DeNoising Anchor Boxes for End-to-End Object Detection. In *arXiv preprint arXiv:2203.03605*, 2022.
- [14] Yian Zhao, Wenyu Lv, Shangliang Xu, Jinman Wei, Guanzhong Wang, Qingqing Dang, Yi Liu, and Jie Chen. DETRs Beat YOLOs on Real-time Object Detection. In *arXiv preprint arXiv:2304.08069*, 2023.
- [15] Ross Girshick, Jeff Donahue, Trevor Darrell, and Jitendra Malik. Rich Feature Hierarchies for Accurate Object Detection and Semantic Segmentation. In *Proceedings of the IEEE conference on computer vision and pattern recognition(CVPR)*, 2014.
- [16] Ross Girshick. Fast R-CNN. In *Proceedings of the IEEE international conference on computer vision(CVPR)*, 2015.
- [17] Shaoqing Ren, Kaiming He, Ross Girshick, and Jian Sun. Faster R-CNN: Towards Real-Time Object Detection with Region Proposal Networks. In *IEEE transactions on pattern analysis and machine intelligence*, 39(6):1137–1149, June 2016.
- [18] Kaiming He, Georgia Gkioxari, Piotr Dollár, and Ross Girshick. Mask R-CNN. In *Proceedings of the IEEE international conference on computer vision(CVPR)*, 2018.
- [19] Zhaowei Cai and Nuno Vasconcelos. Cascade R-CNN: Delving into High Quality Object Detection. In *Proceedings of the IEEE conference on computer vision and pattern recognition(CVPR)*, 2018: 6154-6162.
- [20] Wei Liu, Dragomir Anguelov, Dumitru Erhan, Christian Szegedy, Scott Reed, Cheng-Yang Fu, and Alexander C. Berg. SSD: Single Shot MultiBox Detector. In *Lecture Notes in Computer Science*, pages 21–37. Springer International Publishing, 2016.
- [21] Tsung-Yi Lin, Priya Goyal, Ross Girshick, Kaiming He, and Piotr Dollár. Focal Loss for Dense Object Detection. In *arXiv preprint arXiv:1708.02002*, 2018.
- [22] Joseph Redmon, Santosh Divvala, Ross Girshick, and Ali Farhadi. You Only Look Once: Unified, Real-Time Object Detection. In *Proceedings of the IEEE conference on computer vision and pattern recognition(CVPR)*, 2016: 779-788.
- [23] Joseph Redmon and Ali Farhadi. YOLO9000: Better, Faster, Stronger. In *Proceedings of the IEEE conference on computer vision and pattern recognition(CVPR)*, 2017: 7263-7271.
- [24] Joseph Redmon and Ali Farhadi. YOLOv3: An Incremental Improvement. In *arXiv preprint arXiv:1804.02767 [cs.CV]*, 2018.
- [25] Alexey Bochkovskiy, Chien-Yao Wang, and Hong-Yuan Mark Liao. YOLOv4: Optimal Speed and Accuracy of Object Detection. In *arXiv preprint arXiv:2004.10934 [cs.CV]*, 2020.
- [26] Xiang Long, Kaipeng Deng, Guanzhong Wang, Yang Zhang, Qingqing Dang, Yuan Gao, Hui Shen, Jianguo Ren, Shumin Han, Errui Ding, and Shilei Wen. PP-YOLO: An Effective and Efficient Implementation of Object Detector. In *arXiv preprint arXiv:2007.12099 [cs.CV]*, 2020.
- [27] Chuyi Li, Lulu Li, Yifei Geng, Hongliang Jiang, Meng Cheng, Bo Zhang, Zaidan Ke, Xiaoming Xu, and Xiangxiang Chu. YOLOv6 v3.0: A Full-Scale Reloading. In *arXiv preprint arXiv:2301.05586 [cs.CV]*, 2023.
- [28] Chien-Yao Wang, Alexey Bochkovskiy, and Hong-Yuan Mark Liao. YOLOv7: Trainable Bag-of-Freebies Sets New State-of-the-Art for Real-Time Object Detectors. In *Proceedings of the IEEE/CVF Conference on Computer Vision and Pattern Recognition (CVPR)*, 2023.
- [29] Chen Wang, Wenqiang He, Yunting Nie, et al. Gold-YOLO: Efficient Object Detector via Gather-and-Distribute Mechanism. In *Advances in Neural Information Processing Systems*, volume 36, 2024.

- [30] Xianzhe Xu, Yiqi Jiang, Weihua Chen, Yilun Huang, Yuan Zhang, and Xiuyu Sun. DAMO-YOLO: A Report on Real-Time Object Detection Design. In *arXiv preprint arXiv:2211.15444v2 [cs.CV]*, 2022.
- [31] Yue Liu, Yunjie Tian, Yuzhong Zhao, Hongtian Yu, Lingxi Xie, Yaowei Wang, Qixiang Ye, Yunfan Liu. VMamba: Visual State Space Model. In *arXiv preprint arXiv:2401.10166*, 2024.
- [32] Albert Gu and Tri Dao. Mamba: Linear-Time Sequence Modeling with Selective State Spaces. In *arXiv preprint arXiv:2312.00752*, 2023.
- [33] Lianghui Zhu, Bencheng Liao, Qian Zhang, Xinlong Wang, Wenyu Liu, Xinggang Wang. Vision Mamba: Efficient Visual Representation Learning with Bidirectional State Space Model. In *arXiv preprint arXiv:2401.09417*, 2024.
- [34] Tao Huang, Xiaohuan Pei, Shan You, Fei Wang, Chen Qian, Chang Xu. LocalMamba: Visual State Space Model with Windowed Selective Scan. In *arXiv preprint arXiv:2403.09338*, 2024.
- [35] Mark Everingham, Luc Van Gool, Christopher K. I. Williams, John Winn, Andrew Zisserman. The Pascal Visual Object Classes (VOC) Challenge. *International Journal of Computer Vision*, 88(2):303-338, 2010.
- [36] Tsung-Yi Lin, Michael Maire, Serge Belongie, Lubomir Bourdev, Ross Girshick, James Hays, Pietro Perona, Deva Ramanan, C. Lawrence Zitnick, Piotr Dollár. Microsoft COCO: Common Objects in Context. In *arXiv preprint arXiv:1405.0312*, 2015.
- [37] Yuxin Fang, Bencheng Liao, Xinggang Wang, Jiemin Fang, Jiyang Qi, Rui Wu, Jianwei Niu, and Wenyu Liu. You Only Look at One Sequence: Rethinking Transformer in Vision through Object Detection. In *arXiv preprint arXiv:2106.00666*, 2021.
- [38] Zixiao Zhang, Xiaoqiang Lu, Guojin Cao, Yuting Yang, Licheng Jiao, and Fang Liu. ViT-YOLO: Transformer-Based YOLO for Object Detection. In *Proceedings of the IEEE/CVF International Conference on Computer Vision Workshops (ICCVW)*, pages 2799-2808, 2021.
- [39] Albert Gu, Karan Goel, and Christopher Ré. Efficiently Modeling Long Sequences with Structured State Spaces. In *arXiv preprint arXiv:2111.00396 [cs.LG]*, 2022.
- [40] Albert Gu, Isys Johnson, Karan Goel, Khaled Saab, Tri Dao, Atri Rudra, and Christopher Ré. Combining Recurrent, Convolutional, and Continuous-time Models with Linear State-Space Layers. In *arXiv preprint arXiv:2110.13985 [cs.LG]*, 2021.
- [41] Jimmy T. H. Smith, Andrew Warrington, and Scott W. Linderman. Simplified State Space Layers for Sequence Modeling. In *arXiv preprint arXiv:2208.04933 [cs.LG]*, 2023.
- [42] Glenn Jocher, Ayush Chaurasia, and Jing Qiu. Ultralytics YOLO: Software for Object Detection. Version 8.0.0, January 2023. Available from <https://github.com/ultralytics/ultralytics>.
- [43] Yanyu Li, Ju Hu, Yang Wen, Georgios Evangelidis, Kamyar Salahi, Yanzhi Wang, Sergey Tulyakov, and Jian Ren. Rethinking Vision Transformers for MobileNet Size and Speed. In *Proceedings of the IEEE International Conference on Computer Vision*, 2023.
- [44] Yann N. Dauphin, Angela Fan, Michael Auli, and David Grangier. Language Modeling with Gated Convolutional Networks. In *arXiv preprint arXiv:1612.08083 [cs.CL]*, 2017.
- [45] Abhishek Rajagopal and Vidhyapriya Nirmala. Convolutional Gated MLP: Combining Convolutions and gMLP. In International Conference on Big Data, Machine Learning, and Applications, Singapore: Springer Nature Singapore, pages 721–735, 2021.
- [46] Ultralytics. Ultralytics/yolov5: v7.0 - YOLOv5 SOTA Realtime Instance Segmentation. GitHub repository, Version v7.0, 2022. <https://github.com/ultralytics/yolov5.com>.
- [47] Yuming Chen, Xinbin Yuan, Ruiqi Wu, Jiabao Wang, Qibin Hou, and Ming-Ming Cheng. YOLO-MS: Rethinking Multi-Scale Representation Learning for Real-time Object Detection. In *arXiv preprint arXiv:2308.05480 [cs.CV]*, 2023.
- [48] Ao Wang, Hui Chen, Lihao Liu, Kai Chen, Zijia Lin, Jungong Han, and Guiguang Ding. YOLOv10: Real-Time End-to-End Object Detection. In *arXiv preprint arXiv:2405.14458 [cs.CV]*, 2024.
- [49] Weihao Yu and Xinchao Wang. MambaOut: Do We Really Need Mamba for Vision? In *arXiv preprint arXiv:2405.07992 [cs.CV]*, 2024.
- [50] Hongyi Zhang, Moustapha Cisse, Yann N. Dauphin, and David Lopez-Paz. Mixup: Beyond Empirical Risk Minimization. In *arXiv preprint arXiv:1710.09412*, 2017.
- [51] Ramprasaath R. Selvaraju, Michael Cogswell, Abhishek Das, Ramakrishna Vedantam, Devi Parikh, and Dhruv Batra. Grad-CAM: Visual Explanations from Deep Networks via Gradient-Based Localization. In *Proceedings of the IEEE International Conference on Computer Vision (ICCV)*, pages 618-626, Venice, Italy, October 2017.

- [52] Lin T Y, Dollár P, Girshick R, et al. Feature Pyramid Networks for Object Detection. In *Proceedings of the IEEE Conference on Computer Vision and Pattern Recognition*, 2017, pp. 2117-2125.
- [53] Jiacheng Ruan and Suncheng Xiang. VM-UNet: Vision Mamba UNet for Medical Image Segmentation. In *arXiv preprint arXiv:2402.02491 [eess.IV]*, 2024.
- [54] Jinhong Wang, Jintai Chen, Danny Chen, and Jian Wu. Large Window-based Mamba UNet for Medical Image Segmentation: Beyond Convolution and Self-attention. In *arXiv preprint arXiv:2403.07332 [cs.CV]*, 2024.
- [55] Weibin Liao, Yinghao Zhu, Xinyuan Wang, Chengwei Pan, Yasha Wang, and Liantao Ma. LightM-UNet: Mamba Assists in Lightweight UNet for Medical Image Segmentation. In *arXiv preprint arXiv:2403.05246 [eess.IV]*, 2024.
- [56] Qinfeng Zhu, Yuanzhi Cai, Yuan Fang, Yihan Yang, Cheng Chen, Lei Fan, and Anh Nguyen. Samba: Semantic Segmentation of Remotely Sensed Images with State Space Model. In *arXiv preprint arXiv:2404.01705 [cs.CV]*, 2024.
- [57] Xianping Ma, Xiaokang Zhang, and Man-On Pun. RS3Mamba: Visual State Space Model for Remote Sensing Images Semantic Segmentation. In *arXiv preprint arXiv:2404.02457 [cs.CV]*, 2024.
- [58] Chengqi Lyu, Wenwei Zhang, Haian Huang, Yue Zhou, Yudong Wang, Yanyi Liu, Shilong Zhang, and Kai Chen. RTMDet: An Empirical Study of Designing Real-Time Object Detectors. In *arXiv preprint arXiv:2212.07784 [cs.CV]*, 2022.
- [59] Jiangning Zhang, Xiangtai Li, Jian Li, Liang Liu, Zhucun Xue, Boshen Zhang, Zhengkai Jiang, Tianxin Huang, Yabiao Wang, and Chengjie Wang. Rethinking Mobile Block for Efficient Attention-Based Models. In *2023 IEEE/CVF International Conference on Computer Vision (ICCV)*, pages 1389–1400. IEEE Computer Society, 2023.
- [60] Ao Wang, Hui Chen, Zijia Lin, Hengjun Pu, and Guiguang Ding. RepViT: Revisiting Mobile CNN from ViT Perspective. In *arXiv preprint arXiv:2307.09283*, 2023.
- [61] Sachin Mehta and Mohammad Rastegari. MobileViT: Light-Weight, General-Purpose, and Mobile-Friendly Vision Transformer. In *arXiv preprint arXiv:2110.02178*, 2021.
- [62] Zekai Chen, Fangtian Zhong, Qi Luo, Xiao Zhang, and Yanwei Zheng. EdgeViT: Efficient Visual Modeling for Edge Computing. In *International Conference on Wireless Algorithms, Systems, and Applications*, pages 393–405. Springer, 2022.
- [63] Chien-Yao Wang, Hong-Yuan Mark Liao, Yueh-Hua Wu, Ping-Yang Chen, Jun-Wei Hsieh, and I-Hau Yeh. CSPNet: A New Backbone That Can Enhance Learning Capability of CNN. In *Proceedings of the IEEE/CVF Conference on Computer Vision and Pattern Recognition Workshops*, pages 390–391, 2020.

A Visualization

A.1 Visualization of the Grad-CAM

We used the Grad-CAM[51] visualization approach to compare Mamba YOLO-T and state-of-the-arts in the backbone part, and as can be observed from Figure 6, no matter how the size scale of the object varies, our proposed Mamba YOLO-T assigns higher weights to the detection area of the target, and maintains higher sensitivity to the object location. Position also maintains higher sensitivity, thanks to the clever design of the mamba framework and LS Block, the detector can effectively capture the local and global fusion features of the position information of objects of different sizes.

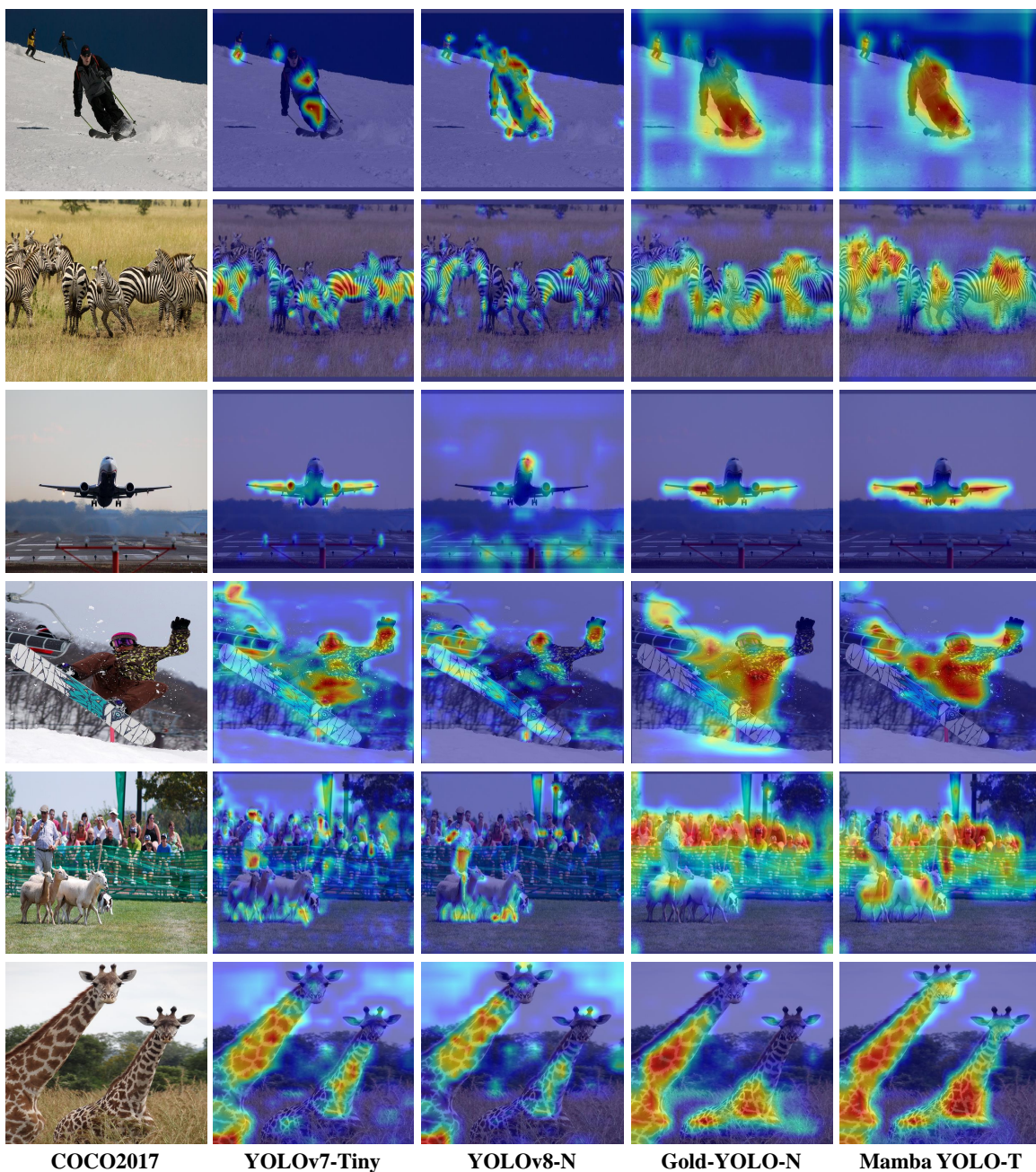


Figure 6: CAM visualization results of YOLOv7-Tiny[28], YOLOv8-N[42], Gold YOLO-N[29], and Mamba YOLO-T in backbone.

A.2 Visualization of the feature maps output by random initial weights

In order to evaluate the ability of the backbone network under the mamba-based architecture in Mamba YOLO to retain boundary information, we used a feature map visualization with random initial weight output. In Figure 7, it can be observed that at the initial stage 0, 1, the backbone network of each detector retains fairly complete information. As the depth increases, especially in stages 3, 4, some of these detectors are no longer able to retain the original information effectively. Among them, the feature maps of YOLOv5 and YOLOv6 behave very blurred, and all distinguishable features are lost, while the feature maps of Mamba YOLO maintain clear boundaries, and the features of recognizable objects are preserved to a certain extent even at the deepest stage 4.

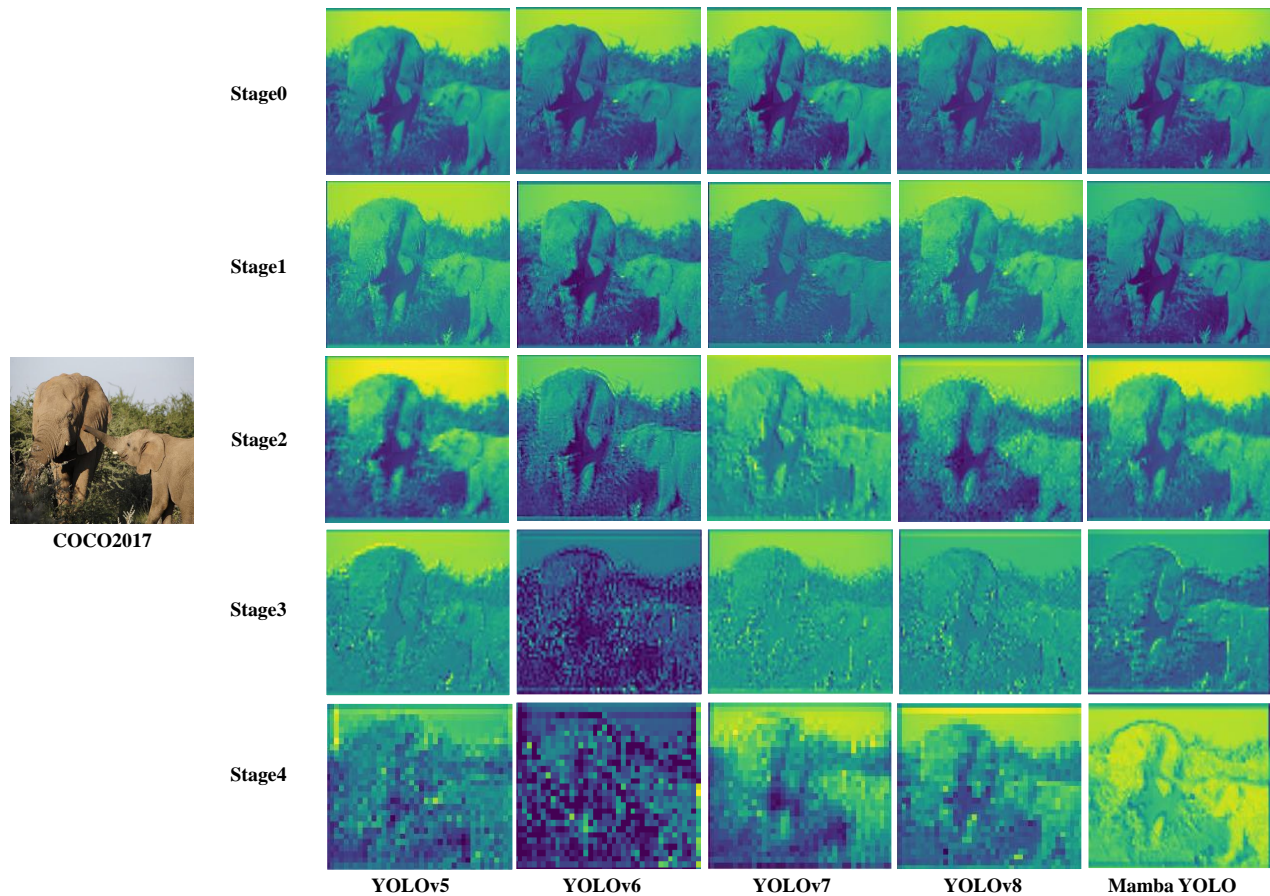


Figure 7: Feature maps output by random initial weights visualization results of YOLOv5[46], YOLOv6[27], YOLOv7[28], YOLOv8[42], and Mamba YOLO in backbone.

A.3 Visualization of detect and segment

Figure 8 shows the visualization results of Mamba YOLO-T’s object detection and instance segmentation on the COCO 2017 validation set, and it can be seen that Mamba YOLO-T can achieve accurate detection under a variety of difficult conditions, and also shows great capability in segmenting a variety of highly overlapping and heavily occluded objects with complex backgrounds.

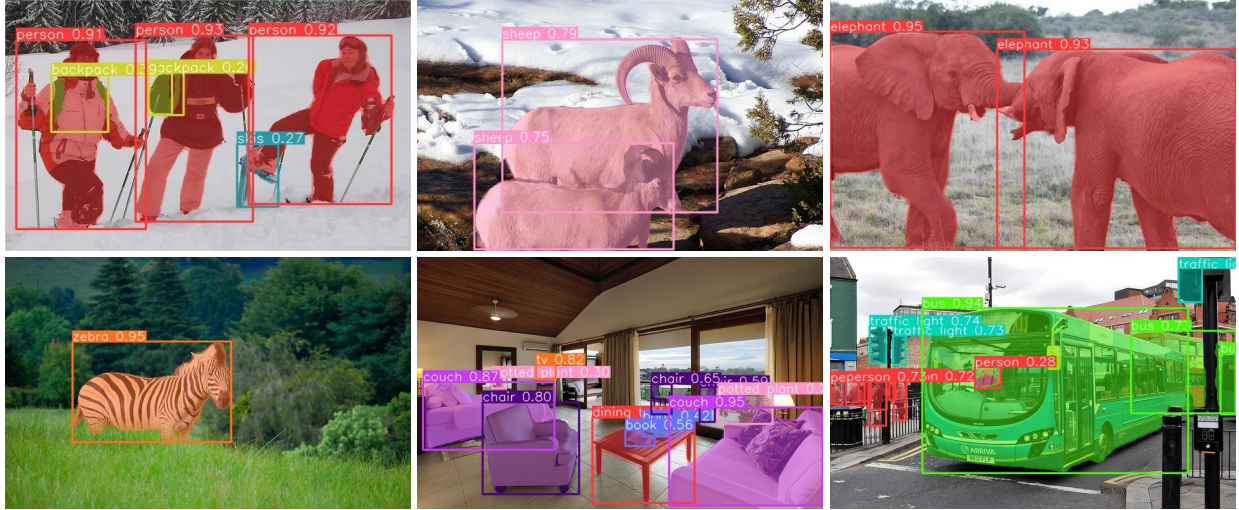


Figure 8: Inference results on the COCO dataset.

B Hyper parameter settings

The training parameters for Mamba YOLO are shown in Table 5. We propose that Mamba YOLO of all sizes was trained using a training strategy from scratch without any pre-training weights for a total of 500 epochs. The strong data augmentation method we used was Mosaic[46, 25] and Mixup[50], the data augmentation operation was turned off at the last 10 epochs.

Table 5: Hyper parameter settings of Mamba YOLO

Hyper Parameter	Value
epochs	500
optimizer	SGD
optimizer weight decay	0.0005
initial learning rate	0.01
final learning rate	0.01
imgsz	640
box loss gain	7.5
cls loss gain	0.5
dfl loss gain	1.5
warmup_epochs	3.0
warmup_momentum	0.8
warmup_bias_lr	0.1
mosaic augmentation	1.0
image HSV-Saturation augmentation	0.7
image HSV-Value augmentation	0.4
image HSV-Hue augmentation	0.015